Metal Fragment Addition and Substitution Reactions of $[Ru_3(CO)_9BH_5]$ and $[Ru_3H(CO)_9(B_2H_5)]$: Molecular Structures of $[WRu_3(cp)H(CO)_{11}(BH)]$ and $[MoRu_3(cp)H_3(CO)_{11}]$ (cp = η-C_5H_5)†

Catherine E. Housecroft,*[a] Dorn M. Matthews,[a] Arnold L. Rheingold*[b] and Xuejing Song[a]

[a] *University Chemical Laboratory, Lensfield Road, Cambridge CB2 1EW, UK*

[b] *Department of Chemistry, University of Delaware, Newark, DE 19716, USA*

The photochemical reactions of $[\{M(cp)(CO)_3\}_2]$ (M = Mo or W, cp = η-C_5H_5) with $[Ru_3(CO)_9BH_5]$ **1** or $[Ru_3H(CO)_9(B_2H_5)]$ **2** have been investigated. The observed cluster products arise by either the addition of a $\{(cp)M(CO)_2\}$ fragment to the Ru_3B cluster core of **1** with associated hydrogen loss or by substitution of one $\{(cp)M(CO)_2\}$ for a $\{BH_2\}$ fragment in either **1** or **2** and, for M = W only, by the substitution of two $\{BH_2\}$ fragments. An assessment as to whether the reaction pathways may be reasonably described in terms of isolobal fragment replacements is presented; Fenske–Hall quantum-chemical calculations are used to show that some degree of semi-bridging character from the Group 6 metal carbonyl ligands to the triruthenium framework necessarily follows as the $\{(cp)M(CO)_2\}$ (M = Mo or W) fragment is introduced in place of the $\{BH_2\}$ unit in **1**. Two products have been characterized by single-crystal X-ray crystallography: $[MoRu_3(cp)H_3(CO)_{11}]$ **4**, monoclinic, space group $P2_1/c$, a = 16.668(5), b = 14.575(6), c = 18.319(4) Å, β = 102.85(2)°, Z = 8; $R(F)$ = 0.0408; $[WRu_3(cp)H(CO)_{11}(BH)]$ **5**, monoclinic, space group $P2_1/c$, a = 17.328(6), b = 7.641(3), c = 17.924(8) Å, β = 114.92(3)°, Z = 4, $R(F)$ = 0.1210. Compound **4** exhibits a tetrahedral metal core and is related to **1** by the replacement of an apical $\{BH\}$ unit and one *endo*-hydrogen atom by a $\{(cp)Mo(CO)_2\}$ group. Compound **5** consists of a butterfly framework of metal atoms with the tungsten atom occupying a wingtip site and is the first heterometallic butterfly cluster containing a semi-interstitial boron atom to be structurally characterized. Partial structural data have been obtained for a third product, $[W_2Ru_3(cp)_2(CO)_{13}]$ and the presence of a trigonal bipyramidal cluster core with two equatorial tungsten sites has been confirmed. This isomer is found not to be that which is dominant in solution.

There are, as yet, very few examples of metal-rich metallaborane clusters which incorporate heterometallic cages and which illustrate a single boron atom interacting with more than one type of transition metal.[1] The study of heterometallic clusters is of interest because the introduction of a heterometal atom or atoms should significantly alter the electronic structure of the metal cage with respect to a homometallic analogue.[2] In particular, if a main-group atom is associated with the metal cage, the reactivity of this atom should be perturbed by a change in the electronic properties of the metal framework. A general strategy for constructing mixed-metal cages around a main-group atom is seen in the transformation of a cluster with a tetrahedral core of type M_3E to a butterfly cluster with core type $M_3M'E$ (M or M′ = transition metal, E = main-group element). Examples so far reported include the formation of the carbide species $[Fe_3Rh(CO)_{12}C]^-$,[2,3] $[Fe_3Mn(CO)_{13}C]^-$,[2,3] $[Fe_3Cr(CO)_{13}C]^{2-}$,[2,4,5] $[Fe_3W(CO)_{13}C]^{2-}$,[2,4,5] $[Ru_3Mn(CO)_{13}C]^-$,[6] and $[Os_3Mn(CO)_{13}C]^-$,[7] the oxide cluster $[Fe_3Mn(CO)_{12}O]^-$,[7] and recently, the boron-containing species $[Ru_3FeH(CO)_{12}(BH_2)]$ and its conjugate base $[Ru_3FeH(CO)_{12}(BH)]^-$.[8]

The synthesis of $[Ru_3FeH(CO)_{12}(BH)]^-$ involves the reaction of $[Ru_3(CO)_9BH_4]^-$ with $[Fe(CO)_5]$ and is similar to the cluster expansion from $[Fe_3(CO)_9BH_4]^-$ to $[Fe_4H(CO)_{12}(BH)]^-$ which uses $[Fe_2(CO)_9]$ as a source of an $\{Fe(CO)_3\}$ fragment.[9,10] Our recent work with the ruthenium/iron system illustrated that reactions of the anionic cluster $[Ru_3(CO)_9BH_4]^-$ with $[Fe(CO)_5]$ gave moderately poor yields of the heterometallic butterfly product. On the other hand, the photolysis of neutral $[Ru_3(CO)_9BH_5]$[11] **1** with $[Fe(CO)_5]$ gave neutral $[Ru_3FeH(CO)_{12}(BH_2)]$ in ≈60% yield (Scheme 1).[8] Although the introduction of the iron atom breaks the symmetry of the butterfly with respect to the all-ruthenium analogue $[Ru_4H(CO)_{12}(BH_2)]$,[8,12–14] it does not alter the environment about the boron atom with respect to the number of associated hydrogen atoms since each of the $\{Fe(CO)_3\}$ and $\{Ru(CO)_3\}$ cluster units provides two cluster-bonding electrons.

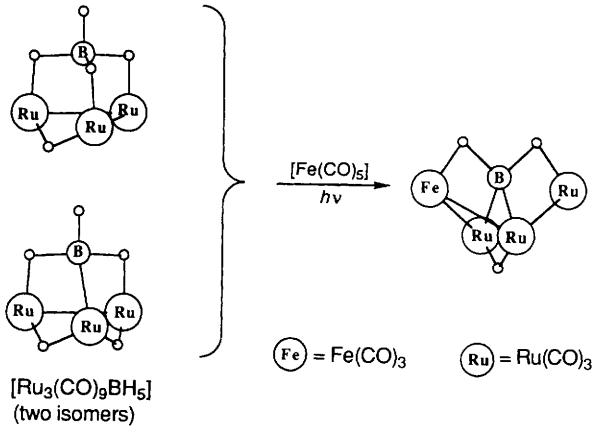

Scheme 1

† *Supplementary data available:* see Instructions for Authors, *J. Chem. Soc., Dalton Trans.*, 1992, Issue 1, pp. xx–xxv.

One of our prime objectives in generating clusters with a heterometallic core of the type $Ru_3M'B$ is significantly to perturb the environment (and hence the reactivity) of the boron atom compared to the case when M' = Ru. In theory, this can readily be achieved by choosing a metal fragment that does not provide the same number of cluster-bonding electrons as does an $\{Ru(CO)_3\}$ fragment. For example, the $\{(cp)M'(CO)_2\}$ unit (M' = Mo or W, cp = η-C_5H_5) is a source of three electrons.[15] The formal substitution of $\{(cp)M'(CO)_2\}$ for $\{Ru(CO)_3\}$ in $[Ru_4H(CO)_{12}(BH_2)]$ would therefore also require the loss of one hydrogen atom if the cluster electron count is to remain constant and the butterfly structure is to be preserved. Here, we report the results of reactions of **1** with $[\{M(cp)(CO)_3\}_2]$ (M = Mo or W), a source of the $\{(cp)M(CO)_2\}$ fragment, and the closely related reactivity patterns of $[Ru_3H(CO)_9(B_2H_5)]$ **2**.[16,17]

Experimental

General Data.—Fourier-transform NMR spectra were recorded on a Bruker WM 250 or AM 400 spectrometer: ^1H shifts are reported with respect to δ 0 for $SiMe_4$, ^{11}B with respect to δ 0 for $F_3B{\cdot}OEt_2$; all downfield chemical shifts are positive. Infrared spectra were recorded on a Perkin Elmer FT 1710 spectrophotometer, fast atom bombardment (FAB) mass spectra on a Kratos MS 50TC, MS 902 or MS 890 instrument.

All reactions were carried out under argon by using standard Schlenk techniques. Solvents were dried over suitable reagents and freshly distilled under N_2 before use. Separations were carried out by thin-layer plate chromatography with Kieselgel 60-PF-254 (Merck). The compound $[Ru_3(CO)_{12}]$ was prepared from $RuCl_3$ (Johnson-Matthey) by a modification of a standard method.[18] The precursor $[Ru_3(CO)_9BH_5]$ **1**[11] was prepared as previously reported. The salt $[NMe_4][B_3H_8]$ (Alfa-Ventron), $[\{Mo(cp)(CO)_3\}_2]$ and $[\{W(cp)(CO)_3\}_2]$ (Aldrich) were used as received. Photolysis experiments used a mercury high-pressure lamp (Aldrich).

Preparation of $[Ru_3H(CO)_9(B_2H_5)]$ **2**—In the first step of the synthesis of compound **2**, $[Ru(CO)_{12-x}(NCMe)_x]$ (x = 1 or 2) was prepared by the following method, a modification of the literature procedure.[19] In a typical reaction, $[Ru_3(CO)_{12}]$ (320 mg, 0.5 mmol) was dissolved in CH_2Cl_2 (150 cm^3) and MeCN (20 cm^3). The solution was cooled to −78 °C and a solution of Me_3NO (76 mg, 0.5 mmol) in CH_2Cl_2 (5 cm^3) was added dropwise over a period of 10 min. The solution was allowed to warm (over 1 h) to room temperature with constant stirring, changing from yellow to dark orange. An IR spectrum of the crude product showed the presence of both $[Ru_3(CO)_{11}(NCMe)]$ and $[Ru_3(CO)_{10}(NCMe)_2]$.[19] The orange solution was filtered through a short column of silica (to remove Me_3NO) into a flask containing $[NMe_4][B_3H_8]$ (58 mg, 0.5 mmol) previously dissolved in CH_2Cl_2 (5 cm^3). The solution was stirred for a minimum of 2 h and solvent was then removed *in vacuo*. The crude product was redissolved in CH_2Cl_2 (20 cm^3) and acidified by using CF_3CO_2H (1 cm^3). After stirring for 20 min, solvent was removed *in vacuo* and neutral products were extracted with hexanes (5 × 10 cm^3). Separation of the products by TLC eluting with hexanes yielded compound **2** as the second (yellow) fraction in ≈20% yield (the yield is increased by leaving the reaction solution to stir for ≈3 d). **2**: NMR ($CDCl_3$): ^1H (400 MHz), δ +4.5 (br, 2 H, BH_{term}), −1.2 (br, 1 H, B–H–B), −12.3 (br, 2 H, Ru–H–B) and −19.0 (s, 1 H, Ru–H–Ru); ^{11}B (128 MHz), δ +17.0 [poorly resolved d, full width at half maximum (f.w.h.m.) 310 Hz; ^{11}B-$\{^1H\}$ f.w.h.m. = 170 Hz, $J_{BH(term)}$ ≈ 120 Hz]. IR (hexane, cm^{-1}): ν_{BH} 2360vw, 2300vw, ν_{CO} 2108w, 2082s, 2061 (sh), 2055vs, 2042m, 2031m, 2012w and 1997w. FAB mass spectrum in 3-nitrobenzyl alcohol matrix: m/z 584 (P^+).

Reaction of Compound **1** *with* $[\{Mo(cp)(CO)_3\}_2]$.—The compound $[\{Mo(cp)(CO)_3\}_2]$ (49 mg, 0.1 mmol) was dissolved in tetrahydrofuran (thf) (1 cm^3) and this solution was added to a solution of **1** (57 mg, 0.1 mmol) in thf (1 cm^3). The reaction mixture was photolysed for 16 h during which time the red solution darkened. The crude mixture was separated by TLC eluting with hexane–CH_2Cl_2 (3:1). The first band to be eluted was yellow and contained unreacted **1**, $[Ru_4H(CO)_{12}(BH_2)]$,[8,12–14] and $[Ru_4H_4(CO)_{12}]$. The second (orange) band consisted of $[MoRu_3(cp)H(CO)_{11}(BH)]$ **3** (≈2% yield) and the third (orange) band was identified as $[MoRu_3(cp)H_3(CO)_{11}]$ **4** (≈20% yield). Compound **3**: NMR (298 K, $CDCl_3$): ^1H (250 MHz), δ +5.28 (s, 5 H, cp), −7.6 (br, q, J_{BH} ≈ 65, 1 H, Ru–H–B) and −20.4 (s, 1 H, Ru–H–Ru); ^{11}B (128 MHz), δ +126.7 (d, J_{BH} = 65 Hz). IR (hexane, cm^{-1}): ν_{CO} 2089w, 2054s, 2021m, 1993w and 1915w. FAB mass spectrum: m/z 785 (P^+). Compound **4**: 250 MHz ^1H NMR (298 K, $CDCl_3$), δ +5.20 (s, 5 H, cp) and −17.0 (s, 3 H). IR (hexane, cm^{-1}): ν_{CO} 2092w, 2061vs, 2056s, 2031m, 2020m, 2012m and 2000w. FAB mass spectrum: m/z 775 (P^+).

Reaction of Compound **1** *with* $[\{W(cp)(CO)_3\}_2]$.—The compound $[\{W(cp)(CO)_3\}_2]$ (67 mg, 0.1 mmol) was dissolved in thf (1 cm^3) and added to a solution of **1** (55 mg, 0.1 mmol) in thf (1 cm^3). The reaction mixture was photolysed for 16 h changing from pink-red to dark red-orange. The crude mixture was separated by TLC eluting with hexane–CH_2Cl_2 (2:1). The first (yellow) band to be eluted consisted of **1**, $[Ru_4H(CO)_{12}(BH_2)]$,[8,12–14] and $[Ru_4H_4(CO)_{12}]$. The second (orange) band was $[WRu_3(cp)H(CO)_{11}(BH)]$ **5** (≈20% yield), the third (orange) fraction was $[WRu_3(cp)H_3(CO)_{11}]$ **6** (≈10% yield), and the final (dark brown) band was $[W_2Ru_3(cp)(CO)_{13}]$ **7** (≈10% yield). Compound **6** was identified after a comparison of spectroscopic data with those in the literature.[20] Compound **5**: NMR (298 K, $CDCl_3$), ^1H (250 MHz), δ +5.30 (s, 5 H, cp), −6.6 (br, q, J_{BH} ≈ 65, 1 H, Ru–H–B) and −20.4 (s, 1 H, Ru–H–Ru); ^{11}B (128 MHz), δ +131.9 (d, J_{BH} = 65 Hz). IR (hexane, cm^{-1}): ν_{CO} 2091m, 2058s, 2049m, 2027s, 1999m, 1989m, 1974m and 1920w. FAB mass spectrum: m/z 874 (P^+). Compound **7**: 250 MHz ^1H NMR (298 K, $CDCl_3$), δ +5.55 (s, 5 H, cp) and +5.50 (s, 5 H, cp). IR (CH_2Cl_2, cm^{-1}): ν_{CO} 2082w, 2073m, 2067w, 2054vs, 2031w, 2025w, 2019m, 2005m, 1997w, 1986s, 1972m, 1952w, 1940w, 1860w and 1838w. FAB mass spectrum: m/z (1165 (P^+).

Reaction of Compound **2** *with* $[\{Mo(cp)(CO)_3\}_2]$.—Compound **2** (12 mg, 0.02 mmol) was dissolved in thf (0.5 cm^3) and a solution of $[\{Mo(cp)(CO)_3\}_2]$ (10 mg, 0.02 mmol) in thf (0.5 cm^3) was added. The reaction mixture was photolysed for 16 h, remaining dark red. The products were separated by TLC eluting with hexane–CH_2Cl_2 (3:1). The first fraction to be eluted was yellow and consisted of $[Ru_4H_4(CO)_{12}]$ with traces of unreacted **2** and of $[Ru_4H(CO)_{12}(BH_2)]$.[8,12–14] The major product (≈10% yield) was eluted as the second (orange) band and was identified as **3** (see above). Several other products were produced in trace amounts but were not characterized.

Reaction of Compound **2** *with* $[\{W(cp)(CO)_3\}_2]$.—Compound **2** (12 mg, 0.02 mmol) was dissolved in thf (0.5 cm^3) and a solution of $[\{W(cp)(CO)_3\}_2]$ (10 mg, 0.02 mmol) in thf (0.5 cm^3) was added. The reaction mixture was photolysed for 16 h changing from pink-red to burgundy-red. Products were separated by TLC eluting with hexane–CH_2Cl_2 (3:1). The first fraction to be eluted was yellow and consisted of $[Ru_4H_4(CO)_{12}]$ with minor amounts of unreacted **2** and of $[Ru_4H(CO)_{12}(BH_2)]$.[8,12–14] The second (orange) fraction (≈30% yield) was **5**, the third (orange, ≈10% yield) was identified as **6**, and the fourth (dark brown, ≈25% yield) was **7**.

Crystal Structural Determinations.—General data. Crystallo-

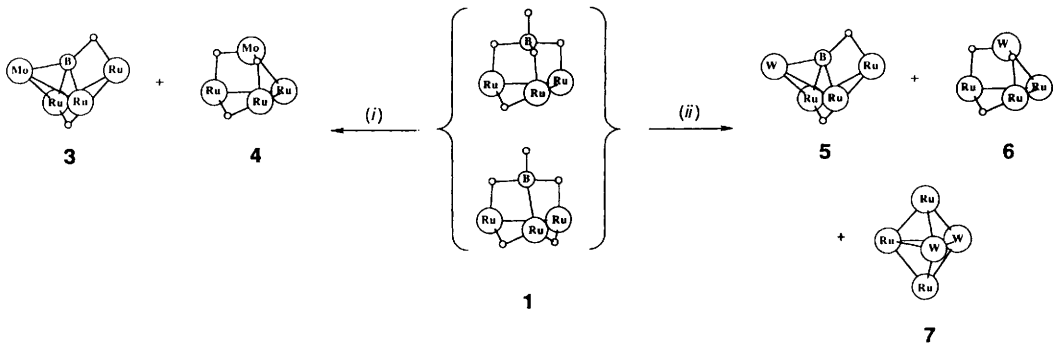

Scheme 2 (*i*) $[\{Mo(cp)(CO)_3\}_2]$, *hv*, thf, 16 h; (*ii*) $[\{W(cp)(CO)_3\}_2]$, *hv*, thf, 16 h

graphic data for compounds **4** and **5** are collected in Table 1. Photographic characterization of both compounds revealed $2/m$ Laue symmetry, and systematic absences in the diffraction data uniquely determined the space groups.

All specimens of compound **5** diffracted broadly and weakly, and produced very distorted peak shapes with unbalanced backgrounds. This resulted in the rejection of 217 reflections for background imbalance. Additionally, axial photographs contained numerous weak interlayer spots (the *z* axis being the most notably affected) suggesting that, in addition to possible twinning problems, there also existed the presence of a superlattice. However, no reflections of significant intensity attributable to a superlattice were observed, which is not uncommon given the domination of all diffraction by the sub-lattice. We have chosen to report this structure in its sub-lattice form, which clearly makes it of low quality, because we are confident that the framework is correct and that it serves to identify the chemical nature of **5**. As a consequence of these circumstances, the lighter-atom bond metrics are not considered to be reliable.

Corrections for absorption were applied by empirical ψ-scan methods. The structures were solved by direct methods which located the heavy atoms in each structure. In **4** all non-hydrogen atoms were refined with anisotropic thermal parameters and hydrogen atoms were treated as idealised contributions. In **5** only the metal and oxygen atoms were anisotropically refined and the hydrogen atoms were ignored. Maximum residual electron density for **4** is 0.76 e $Å^{-3}$ located 1.02 Å from Ru(3); for **5** it is 5.39 e $Å^{-3}$ located 1.02 Å from W. All computations and sources or scattering factors were obtained from the SHELXTL library.[21]

Additional material available from the Cambridge Crystallographic Data Centre comprises H-atom coordinates, thermal parameters and remaining bond lengths and angles.

Molecular Orbital Calculations.—Fenske–Hall calculations[22] were carried out on the compound $[MoRu_3(cp)H_3(CO)_{11}]$ **4** in terms of orbital interactions between the fragments $[Ru_3H_3(CO)_9]$ and $[Mo(cp)(CO)_2]^+$. The geometry was based on the structure of $[WRu_3(\eta\text{-}C_5Me_5)H_3(CO)_{11}]$ for which H atoms were located directly by X-ray crystallography.[20] The frontier molecular orbitals of $\{BH_2\}^+$ were also generated for comparison with those of $\{(cp)Mo(CO)_2\}^+$. The $\{BH_2\}^+$ fragment has C_s symmetry since one H atom is potentially a bridging atom and one a terminal atom ($d_{BH(term)} < d_{BH(br)}$). The calculations employed single-ζ Slater functions for the 1s and 2s orbitals of B, C and O. Exponents were obtained by curve fitting the double-ζ functions of Clementi[23] while maintaining orthogonal functions. Double-ζ functions were used directly for the 2p orbitals. An exponent of 1.16 was used for H. The Ru and Mo atoms[24] were augmented by 5s and 5p functions with exponents of 2.20. Fragment orbital energies (see Fig. 5) were taken from the Fock matrix of the final complex.[25]

Results and Discussion

Reaction of Compound **1** *with* $[\{M(cp)(CO)_3\}_2]$ (M = Mo *or* W).—In the reaction of $[\{M(cp)(CO)_3\}_2]$ with compound **1** our expectation was that if the pathway paralleled that of $[Fe(CO)_5]$ with **1** the products would be $[MoRu_3(cp)H(CO)_{11}(BH)]$ and $[WRu_3(cp)H(CO)_{11}(BH)]$ respectively. In fact we found that the reaction of **1** with $[\{Mo(cp)(CO)_3\}_2]$ proceeds by the two competing routes shown in Scheme 2. The first is as expected, the addition of the heterometallic fragment to cluster **1** with concomitant loss of hydrogen to give $[MoRu_3(cp)H(CO)_{11}(BH)]$ **3**. The second path may be described as substitution of the boron vertex in **1** by a molybdenum fragment to give $[MoRu_3(cp)H_3(CO)_{11}]$ **4**. The reaction of **1** with $[\{W(cp)(CO)_3\}_2]$ is more complex and three pathways compete with one another (Scheme 2). Two mimic their molybdenum counterparts to generate $[WRu_3(cp)H(CO)_{11}(BH)]$ **5** and $[WRu_3(cp)H_3(CO)_{11}]$ **6** respectively while the third route leads to $[W_2Ru_3(cp)_2(CO)_{13}]$ **7**.

The conversions of compound **1** into **3** or **5** represent cluster-capping reactions. The $\{(cp)M'(CO)_2\}$ fragment (M′ = Mo or W) caps one Ru_2B face of the initial Ru_3B cluster core. During this step the boron atom is transformed[9] from a vertex group carrying a terminal hydrogen atom *via* a localized two-centre two-electron bond to a semi-interstitial atom for which all valence electrons are available for cluster bonding. The excess of cluster electrons thereby created is removed in associated hydrogen loss as in the formation of $[Ru_3FeH(CO)_{12}(BH_2)]$ shown in Scheme 1. The transformations of **1** to **4** or **6** are simply rationalized in terms of the isolobal replacement of a $\{BH_2\}$ group for a $\{(cp)M'(CO)_2\}$ cluster fragment. This idea is discussed in more detail in a later section.

Although a cluster model of bonding appears to be a useful concept when considering the transformations of compound **1** into **3**, **4**, **5** or **6**, it is more difficult to visualize the conversion of **1** into **7** within this bonding description. It is possible to describe the conversion in terms of a combination of (*i*) a W-for-B substitution and (*ii*) a tungsten-capping reaction. However, this seems to be rather clumsy and it is more convenient to consider the borane unit in **1** as a ligand rather than as an integral part of the cluster. Thus, taking the $\{BH_4\}$ ligand as a five-electron donor, its complete removal would leave a 43-electron 'super-unsaturated' $\{HRu_3(CO)_9\}$ framework. Obviously, this degree of unsaturation may be tuned by encouraging a greater or lesser loss of H atoms. For example, further H loss provides a 42-electron trimetal framework and the formation of **7** is readily understood in terms of the addition of $[(cp)W(CO)_2]_2$ to the

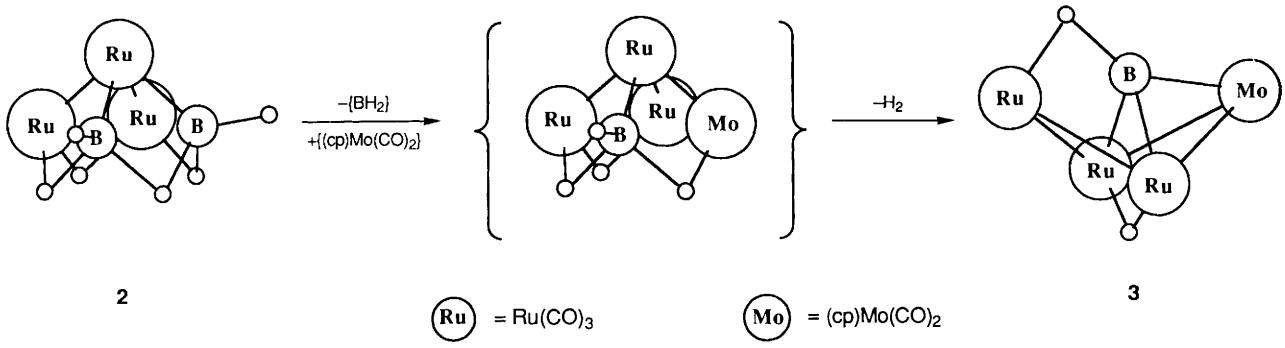

Scheme 3

latter. A partial structural determination* of **7** confirms its trigonal-bipyramidal core, but illustrates that the two tungsten atoms occupy equivalent equatorial sites. This parallels the arrangement of the metal atoms in the related $[Mo_2Os_3(cp)_2H_2(CO)_{12}]$ in which the two molybdenum atoms occupy two equatorial sites of a trigonal-bipyramidal framework.[26] The solution properties of **7** are discussed further below.

The change in bonding model for the borane unit in compound **1** from a cluster fragment to a ligand may appear to be a subtle one but it highlights the fact that one concept alone may not always be appropriate or convenient for all discussions of the structure or chemical reactivity of metalloboranes.[27] A similar dual approach is useful for cluster **2** as illustrated below. Significantly, if the cluster model is deemed appropriate in discussing the conversion of **1** into **7**, one consequence is that compound **6** should be an intermediate along the reaction pathway. If the ligand model is seen as appropriate, then the formation of **6** is not required. In order to test this, we have attempted to convert **6** into **7** *via* the photolysis of **6** with $[\{W(cp)(CO)_3\}_2]$ in thf. This transformation does *not* occur under these conditions, *i.e.* the conditions under which **1** *does* react with $[\{W(cp)(CO)_3\}_2]$ to give **7**. This result would tend to indicate that reaction of **1** to form either **6** or **7** occurs *via* loss of the borane moiety and trapping of the Ru_3-based fragment by reaction with either a mono- or di-meric Group 6 metal unit.

Reaction of Compound **2** *with* $[\{M(cp)(CO)_3\}_2]$ (M = Mo *or* W).—Compound **2** may be considered either as an isolobal analogue of B_5H_9 or as comprising a triruthenium framework that supports a diborane ligand.[16] We have recently confirmed this geometry crystallographically in $[Ru_3H(CO)_8(PPh_3)(B_2H_5)]$.[17] In the reaction of **2** with $[\{Mo(cp)(CO)_3\}_2]$, compound **3** is the only cluster produced in any significant amount and the product distribution contrasts with that observed in the reaction of **1** with $[\{Mo(cp)(CO)_3\}_2]$ (Scheme 2). The conversion of **2** into **3** is illustrated in Scheme 3 and may be considered in cluster terms to be an isolobal replacement of one $\{BH_2\}$ by a $\{(cp)Mo(CO)_2\}$ fragment with associated hydrogen loss. The fact that the sequence does not terminate in a square-based pyramidal cluster retaining one BH unit in a vertex site is interesting. Fehlner[28,29] has delineated the series of possible isomers of $[\{Fe(CO)_3\}_nB_{5-n}H_{9-n}]$ which are formally derived from the square-based pyramidal pentaborane(9) precursor. Not all members of this particular ferraborane series are known but other related species allow a progression from borane to metal-rich metallaborane, for example $[Fe(CO)_3(B_4H_8)]$,[30] $[Co(cp)(B_4H_8)]$,[31–34] $[Fe_2(CO)_9(B_3H_7)]$[35,36] and $[Ru_3H(CO)_8L(B_2H_5)]$ (L = CO[16] or PPh_3[17]). However no example of a cluster of the type $[M_4H_2(CO)_{12}(BH_3)]$ has yet been observed. Significantly, dehydrogenated analogues[29] such as $[Fe_4H(CO)_{12}(BH_2)]$,[37,38] $[Ru_4H(CO)_{12}(BH_2)]$[8,12–14] and $[Ru_3FeH(CO)_{12}(BH_2)]$[8] have been characterized and indeed compounds **3** and **5** may also be classed as such analogues. However, each of the latter butterfly clusters has been prepared from lower-nuclearity precursors and hence a description as a 'dehydrogenated derivative of square-pyramidal $[M_4H_2(CO)_{12}(BH_3)]$' might be seen only as a formalism. The reaction of **2** with $[\{Mo(cp)(CO)_3\}_2]$ is an opportunity to begin with a metal-rich metalloborane which is a true isolobal relative of B_5H_9 and perform a formal isolobal fragment substitution in order to see if the elusive $[M_4H_2(CO)_{12}(BH_3)]$ type of compound can be prepared. The answer for this particular reaction appears to be no; we have only observed the dehydrogenated species **3** and we have no evidence for a stable intermediate of the type shown schematically in Scheme 3.

The reaction of compound **2** with $[\{W(cp)(CO)_3\}_2]$ leads to the same three products identified when **1** reacts with the tungsten dimer. The formation of compound **5** parallels that of **3** described in detail above. Within the concept of cluster bonding, the formation of **7** may be envisaged as a double substitution of isolobal $\{BH_2\}$ for $\{(cp)W(CO)_2\}$ fragments. Once again, a square-based pyramidal cluster which would formally be the product of such a substitution {*viz.* $[W_2Ru_3(cp)_2H_2(CO)_{13}]$} is not observed and the dehydrogenated derivative, the closed cluster **7**, is preferentially formed in 25% yield. The formation of **7** may also be rationalized by considering the addition of the tungsten dimer to an unsaturated Ru_3 platform which becomes available *in situ* once the diborane ligand has been removed. As with **1**, we favour this latter description.

A rationalization of the conversion of compound **2** into **6** is not conveniently described within the cluster model since the transformation requires the substitution of *one* tungsten for *two* boron vertices. However, if **2** is considered in terms of a triruthenium framework supporting a diborane ligand, then the concept of ligand removal followed by the addition of the tungsten fragment to the otherwise unsaturated Ru_3 framework provides a reasonable interpretation for the reaction pathway.

Molecular Structure of Compound **4**.—The molecular structure of and labelling scheme for compound **4** are shown in Fig. 1, atomic coordinates are given in Table 2 and selected bond distances and angles for the two independent molecules are listed in Table 3. Compound **4** is a member of a series of the type $[M'M_3H_3L(CO)_{11}]$ in which M′ = Mo or W, M = Ru or Os and L = cp or η^5-C_5Me_5; crystallographic data are available for $[WRu_3(\eta\text{-}C_5Me_5)H_3(CO)_{11}]$,[20] $[WOs_3(cp)H_3(CO)_{11}]$[39,40] and $[MoOs_3(cp)H_3(CO)_{11}]$.[26] These compounds fall into one of the two structural types **I** and **II** shown in Scheme 4 depending upon the positions of the hydride ligands. Cluster **4** exhibits a tetrahedral Ru_3Mo core and is

* A full structural characterisation of small, dark red crystals of compound **7** was attempted, but only about 30% of the unique reflections in the 4–45° (Mo-Kα) sphere were observed. Nonetheless, it was possible to obtain the heavy-atom framework which consists of a trigonal bipyramid with both W atoms in the equatorial plane. A view of the heavy-atom framework and the metal–metal bond distances and angles are given in the Supplementary Material. Other details: monoclinic, space group $P2_1/n$, a = 9.525(6), b = 17.275(8), c = 16.634(8) Å and β = 92.10(3)°

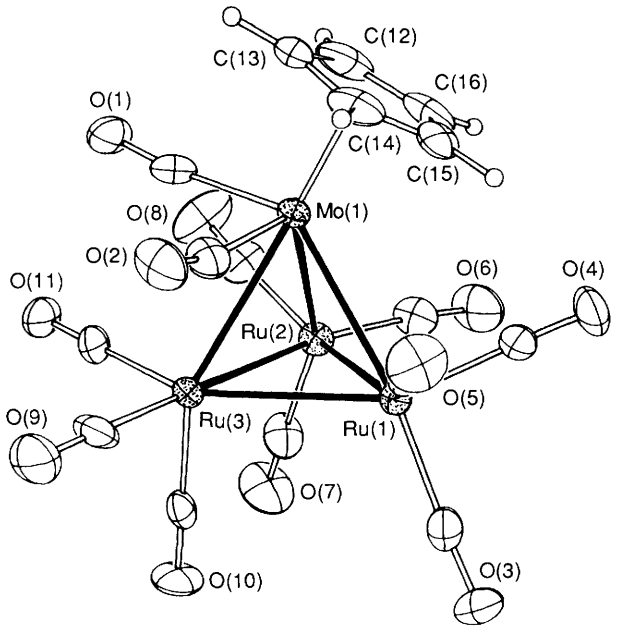

Fig. 1 Molecular structure and labelling scheme for compound **4**

Table 1 Crystallographic data for $[MoRu_3(cp)H_3(CO)_{11}]$ **4** and $[WRu_3(cp)H(CO)_{11}(BH)]$ **5***

	4	**5**
(*a*) Crystal parameters		
Formula	$C_{16}H_8MoO_{11}Ru_3$	$C_{16}H_7BO_{11}Ru_3W$
M	775.38	873.09
a/Å	16.668(5)	17.328(6)
b/Å	14.575(6)	7.641(3)
c/Å	18.319(4)	17.924(8)
β/°	102.85(2)	114.92(3)
U/Å^3	4339(2)	2152.5(18)
F(000)	2928	1608
Z	8	4
Crystal dimensions/mm	0.20 × 0.22 × 0.26	0.18 × 0.24 × 0.42
Crystal colour	Dark red	Orange
D_c/g cm^{-3}	2.374	2.694
μ(Mo-Kα)/cm^{-1}	26.1	77.2
Maximum, minimum transmission	0.48, 0.43	1.00, 0.29
(*b*) Data collection		
2θ scan range/°	4–50	4–46
Data collected (*h*,*k*,*l*)	±20, +18, +22	±20, +9, +20
Reflections collected	7787	3297
Independent reflections	7222	2919
Independent observed reflections [$F_o \geqslant 4\sigma(F_o)$]	4776	2068
(*c*) Refinement		
R(*F*)	0.0408	0.1210
R′	0.0486	0.1275
Δ/σ(max.)	0.053	0.080
Δ(ρ)/e Å^{-3}	0.74	5.40
N_o/N_v	8.54	10.71
Goodness of fit	1.023	2.201

* Details in common: monoclinic, space group $P2_1/c$; *T* 295 K; Nicolet R3 diffractometer; graphite-monochromatized radiation, λ(Mo-Kα) 0.710 73 Å; variation in standards < 1%; N_o = number of observations, N_v = number of variables; weighting scheme, $w^{-1} = \sigma^2(F_o) + 0.001\,F_o^2$.

isomorphous with $[MoOs_3(cp)H_3(CO)_{11}]$.[26] Thus, as with the latter, the tetrametal core of **4** exhibits distortion such that there is one lengthened M–Mo edge and two elongated M–M edges

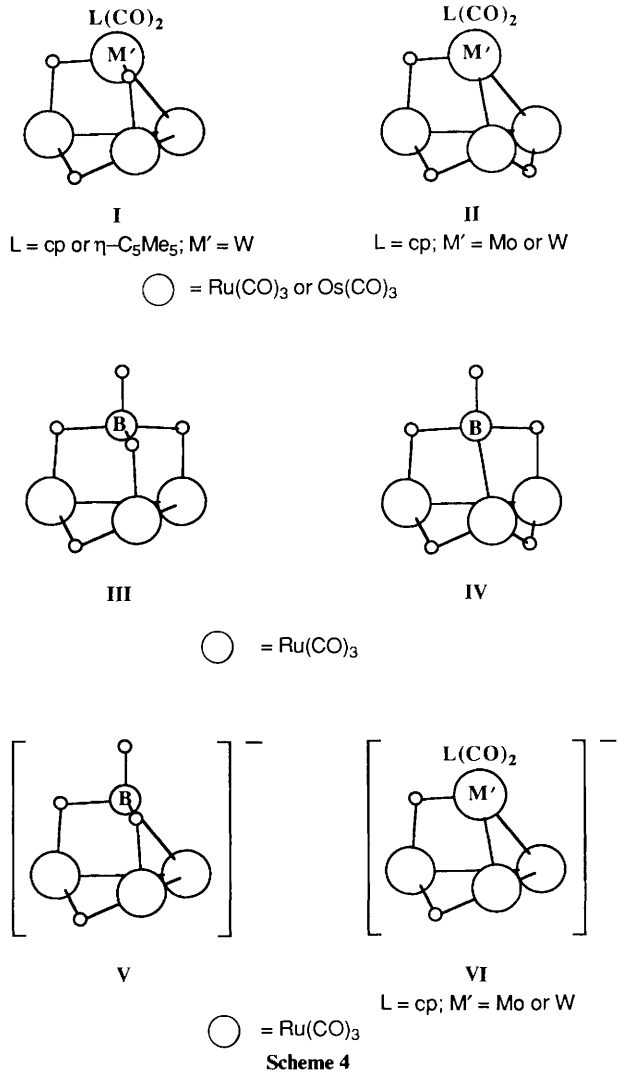

Scheme 4

(M = Ru or Os). Hydrogen atoms were not located directly by X-ray crystallography but the lengthening of specific edges in **4** implies placement of bridging hydrogen atoms along Ru(1)–Ru(2), Ru(1)–Ru(3) and Ru(2)–Mo(1) in molecule A (Fig. 1) and along the equivalent metal–metal bonds Ru(1)–Ru(2), Ru(2)–Ru(3) and Ru(1)–Mo(1) in molecule B.

Solution Properties of Compound **4**.—One feature of interest among compounds in the group $[M'M_3H_3L(CO)_{11}]$ is the presence of the two isomeric forms **I** and **II** (Scheme 4). Chi *et al.*[20] have studied in detail the solution properties of the tungsten-containing members of the series. For $[WRu_3(\eta\text{-}C_5Me_5)H_3(CO)_{11}]$ in CD_2Cl_2 and $[WOs_3(\eta\text{-}C_5Me_5)H_3(CO)_{11}]$ in $CDCl_3$, structure **I** persists in solution with the hydride ligands undergoing exchange. In CD_2Cl_2, $[WRu_3(cp)H_3(CO)_{11}]$ exists as an isomeric mixture of **I** (87) and **II** (13%). For $[WOs_3(cp)H_3(CO)_{11}]$, isomers **I** and **II** are again present but their ratio is critically solvent dependent. Shore and co-workers[26] have reported that, in CD_2Cl_2, $[MoOs_3(cp)H_3(CO)_{11}]$ retains the arrangement of hydrides observed in the solid state, namely structure **I**; the three hydride environments are frozen out at 180 K.

As indicated above, the solid-state structure of compound **4** implies the presence of one Mo–H–Ru and two Ru–H–Ru hydride ligands. The variable-temperature ^1H NMR spectrum of a solution of **4** in CD_2Cl_2 is shown in Fig. 2. At 298 K, **4** exhibits a single sharp resonance in the metal hydride region at δ −17.0. This signal broadens and shifts to higher field as the temperature is lowered and at 184 K it has almost disappeared.

Table 2 Atomic coordinates ($\times 10^4$) for $[MoRu_3(cp)H_3(CO)_{11}]$ **4**

Atom	*x*	*y*	*z*	Atom	*x*	*y*	*z*
Ru(1)	3228.8(5)	1059.3(6)	6643.9(5)	C(13)	6097(7)	1915(8)	7824(8)
Ru(2)	3843.9(5)	1803.7(6)	5390.0(4)	C(14)	5553(7)	1367(10)	8139(6)
Ru(3)	3334.5(5)	3017.7(5)	6379.0(5)	C(15)	5331(7)	636(9)	7698(7)
Ru(1′)	19.6(5)	2948.6(5)	6770.4(4)	C(16)	5685(8)	670(10)	7100(7)
Ru(2′)	−577.9(5)	2175.3(5)	5274.0(4)	O(1′)	−2335(5)	3592(6)	7348(4)
Ru(3′)	−1135.2(5)	1517.9(5)	6575.8(5)	O(2′)	−3077(5)	1730(6)	5510(5)
Mo(1)	4830.9(5)	1963.7(6)	7020.2(4)	O(3′)	1507(5)	1890(6)	7626(5)
Mo(1′)	−1760.4(5)	3272.2(6)	5866.9(4)	O(4′)	1032(5)	4649(6)	6594(5)
O(1)	5646(5)	3748(6)	6594(5)	O(5′)	−434(5)	3450(7)	8238(4)
O(2)	4278(5)	3077(6)	8262(5)	O(7′)	608(6)	881(7)	4721(5)
O(3)	1463(5)	341(7)	6306(6)	O(6′)	−111(5)	3768(6)	4388(5)
O(4)	3961(5)	−832(5)	6503(5)	O(8′)	−2085(5)	1636(6)	4093(5)
O(5)	3444(5)	928(7)	8340(4)	O(9′)	−1746(5)	1716(6)	7997(4)
O(6)	4166(6)	88(7)	4555(6)	O(10′)	266(5)	376(6)	7440(5)
O(7)	2467(6)	2390(8)	4079(5)	O(11′)	−2195(7)	−164(6)	6041(6)
O(8)	5100(6)	2989(7)	4862(5)	C(1′)	−2074(7)	3423(7)	6847(5)
O(9)	2780(5)	4259(7)	7507(6)	C(2′)	−2498(6)	2199(7)	5695(6)
O(10)	1678(4)	3221(6)	5304(4)	C(3′)	939(7)	2257(8)	7298(6)
O(11)	4091(5)	4548(5)	5626(5)	C(4′)	667(6)	4010(7)	6666(6)
C(1)	5290(6)	3119(8)	6715(5)	C(5′)	−269(6)	3287(8)	7682(6)
C(2)	4375(7)	2717(8)	7734(6)	C(7′)	176(7)	1366(8)	4943(5)
C(3)	2110(7)	635(7)	6400(7)	C(6′)	−299(6)	3171(7)	4723(6)
C(4)	3697(6)	−115(8)	6568(6)	C(8′)	−1517(7)	1846(7)	4534(6)
C(5)	3377(6)	982(7)	7701(6)	C(9′)	−1533(7)	1668(7)	7450(6)
C(6)	4076(7)	769(9)	4865(6)	C(10′)	−243(7)	824(7)	7098(7)
C(7)	2969(8)	2181(8)	4598(7)	C(11′)	−1820(8)	462(8)	6240(7)
C(8)	4626(7)	2558(9)	5057(6)	C(12′)	−2751(7)	3806(9)	4875(6)
C(9)	2999(6)	3783(8)	7103(7)	C(13′)	−2845(7)	4244(8)	5515(7)
C(10)	2309(7)	3144(6)	5701(6)	C(14′)	−2140(7)	4803(8)	5773(6)
C(11)	3810(7)	3980(7)	5905(7)	C(15′)	−1619(7)	4667(7)	5269(7)
C(12)	6162(7)	1450(11)	7133(9)	C(16′)	−2006(7)	4073(8)	4699(6)

Table 3 Selected bond distances (Å) and angles (°) for $[MoRu_3(cp)H_3(CO)_{11}]$ **4**

	Molecule A	Molecule B
Ru(1)–Ru(2)	2.924(1)	2.926(1)
Ru(1)–Ru(3)	2.907(1)	2.806(1)
Ru(1)–Mo(1)	2.920(1)	3.095(1)
Ru(2)–Ru(3)	2.796(1)	2.907(1)
Ru(2)–Mo(1)	3.081(1)	2.928(1)
Ru(3)–Mo(1)	2.942(1)	2.951(1)
Ru(2)–Ru(1)–Ru(3)	57.3(1)	60.9(1)
Ru(2)–Ru(1)–Mo(1)	63.6(1)	58.1(1)
Ru(3)–Ru(1)–Mo(1)	60.7(1)	59.8(1)
Ru(1)–Ru(2)–Ru(3)	61.0(1)	57.5(1)
Ru(1)–Ru(2)–Mo(1)	58.1(1)	63.8(1)
Ru(3)–Ru(2)–Mo(1)	59.8(1)	60.8(1)
Ru(1)–Ru(3)–Ru(2)	61.7(1)	61.6(1)
Ru(1)–Ru(3)–Mo(1)	59.9(1)	65.0(1)
Ru(2)–Ru(3)–Mo(1)	64.9(1)	60.0(1)
Ru(1)–Mo(1)–Ru(2)	58.3(1)	58.1(1)
Ru(1)–Mo(1)–Ru(3)	59.5(1)	55.2(1)
Ru(2)–Mo(1)–Ru(3)	55.3(1)	59.3(1)

In three solvents of varying polarity [CD_2Cl_2, $C_4D_{10}O$ and $(CD_3)_2CO$] the resonance remained unchanged (sharp and at δ −17.0 ± 0.1) at 298 K. The facile nature of the exchange process observed for **4** does not permit us to say anything about the static structure nor whether in fact isomers of types **I** and **II** might be present in solution. The barrier to the hydride-exchange process in **4** is lower than is observed for the isomorphous cluster $[MoOs_3(cp)H_3(CO)_{11}]$;[26] this is expected on the grounds of the relative Mo–H–Ru *vs.* Mo–H–Os and Ru–H–Ru *vs.* Os–H–Os bond enthalpies.

The exchange process for compound **4** is also more facile than that observed for $[WRu_3(\eta^5\text{-}C_5Me_5)H_3(CO)_{11}]$, a feature which is again rationalized in terms of relative bond enthalpies, *E*(Mo–H–Ru) *vs.* *E*(W–H–Ru). Proton NMR spectral data for the latter show a single sharp resonance at δ −17.83 at 348 K, a broad signal at δ −18.46 at room temperature and at 235 K two sharp hydride resonances at δ −18.34 (2 H, J_{WH} = 47 Hz) and −18.69 (1 H).[20]

Comparison of $[M'M_3H_3L(CO)_{11}]$ (M′ = Mo *or* W, M = Ru *or* Os, L = cp *or* η-C_5Me_5) *with Compound* **1**.—In discussing the formation of clusters **4** and **6** from **1** we considered the isolobal relationship that exists between a $\{BH_2\}$ fragment and a $\{(cp)M'(CO)_2\}$ fragment (M′ = Mo or W). Compound **1** exists in two isomeric forms, structures **III** and **IV** in Scheme 4.[11] It is gratifying to see that both isomers **I** and **II** are represented amongst members of the isolobal heterometallic clusters $[M'M_3H_3L(CO)_{11}]$ (M′ = Mo or W, M = Ru or Os, L = cp or η-C_5Me_5). The deprotonation of **1** leads to the anion $[Ru_3(CO)_9BH_4]^-$ in which the three bridging hydrogen atoms are fluxional on the ^1H NMR time-scale but for which a static structure of type **V** is proposed.[8] The conjugate bases of both **4** and **6** have been reported[41] and a common structure (**VI**) which mimics that of the isolobally related ruthenaborane anion (**V**) has been proposed.

In replacing a $\{BH_2\}$ unit in compound **1** (see structures **III** and **IV**) by an $\{LM'(CO)_2\}$ fragment (M′ = Mo or W, L = cp or η-C_5Me_5), one bridging hydrogen atom is removed in addition to the substitution of the borane cluster vertex. In the four crystallographically determined structures that are available for members of the $[M'M_3H_3L(CO)_{11}]$ group of compounds, the role of the carbonyl ligands attached to the Group 6 metal varies from terminal to semi-bridging. In $[MoOs_3(cp)H_3(CO)_{11}]$ (isomer **I**) one molybdenum-attached carbonyl ligand is considered by Shore and co-workers[26] to be terminal and the second to be semi-bridging. The same is true in **4** (Fig. 1); the molybdenum carbonyl orientations suggest the evolution of at least one, if not two, semi-bridging interactions with Mo–C–O 171 and 164° in molecule A and 170 and 163° in molecule B. In $[WRu_3(\eta\text{-}C_5Me_5)H_3(CO)_{11}]$ (isomer **II**) both carbonyl ligands associated with the Group 6 metal are

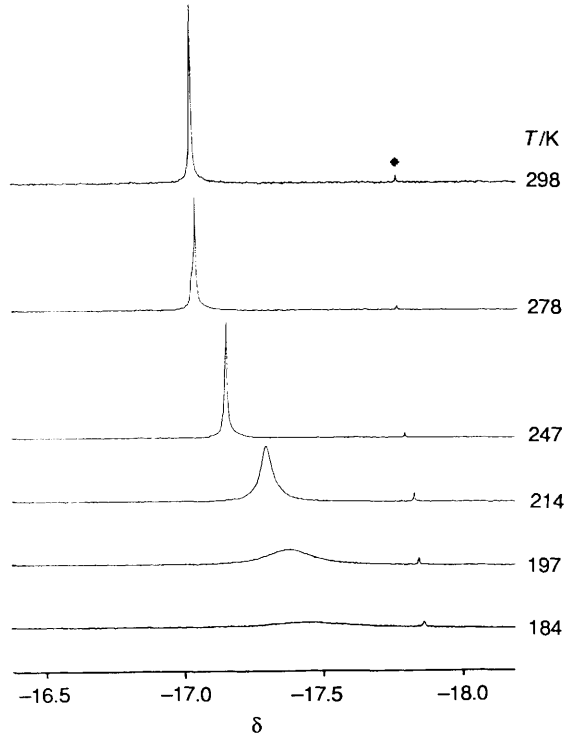

Fig. 2 Variable-temperature 250 MHz ^{1}H NMR spectrum (high-field region only) of compound **4** in CD_2Cl_2. The impurity labelled with an asterisk is $[Ru_4H_4(CO)_{12}]$

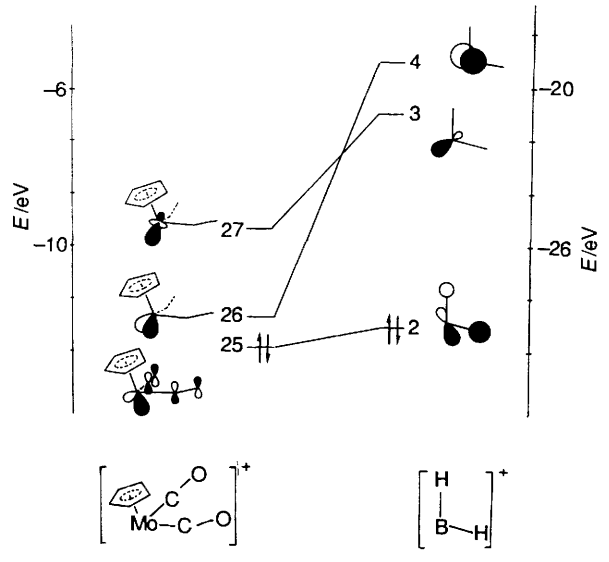

Fig. 3 Comparison of the frontier orbitals of the isolobal fragments $\{(cp)Mo(CO)_2\}^+$ and $\{BH_2\}^+$; eV ≈ 1.60 × 10^{-19} J

described as being terminal,[20] whereas in $[WOs_3(cp)H_3(CO)_{11}]$ (isomer **II**) the carbonyl ligands are considered to be 'terminal or semi-bridging'.[39,40] The absence of semi-bridging interactions in $[WRu_3(\eta\text{-}C_5Me_5)H_3(CO)_{11}]$ has been rationalized in terms of CO ··· C_5Me_5 repulsions.[20]

We considered it worthwhile to compare the frontier-orbital properties of $\{BH_2\}$ and $\{LM'(CO)_2\}$ fragments and to investigate the electronic structure of clusters of the family $[M'M_3H_3L(CO)_{11}]$. One aim was to see whether the semi-bridging interactions observed in some of the latter compounds might in any way be likened to the role of a bridging hydrogen atom in **1**. In Fig. 3 the frontier orbitals of $\{BH_2\}^+$ and $\{(cp)Mo(CO)_2\}^+$ fragments are correlated. A significant feature is the contributions made by the carbon and oxygen 2p atomic orbitals to the composition of MO 25 of the $\{(cp)Mo(CO)_2\}^+$ fragment even though the geometry of the fragment is derived (see Experimental section) from a cluster in which the carbonyl ligands have been described as being terminal.[20] Each carbonyl carbon atom contributes 5% and each oxygen atom 7% towards the composition of MO 25. The MO of the $\{BH_2\}^+$ fragment which correlates with MO 25 of the $\{(cp)Mo(CO)_2\}^+$ fragment contains a 40% contribution from the hydrogen atom which will eventually become the bridging atom in **1**.

A correlation diagram illustrating the interaction of the frontier MOs of the $\{H_3Ru_3(CO)_9\}^-$ and $\{(cp)Mo(CO)_2\}^+$ fragments to form $[MoRu_3(cp)H_3(CO)_{11}]$ **4** is shown in Fig. 4. Since this is a general investigation of clusters of type $[M'M_3H_3L(CO)_{11}]$ we have chosen to use the more symmetrical isomer **I** rather than **II** even though the latter is experimentally determined for **4** in the solid state. The Mulliken overlap populations (MOPs) for the interfragment orbital interactions are listed in Table 4 and the numbers are also expressed as percentages of the total interfragment MOP; overlaps relating to degenerate pairs of MOs (47/48 and 56/57) have been summed together. One of the most striking features is the fact that 28% of the total interfragment MOP is attributed to the interaction between MO 60 of the triruthenium fragment and MO 25 of the $\{(cp)Mo(CO)_2\}^+$ fragment. As the diagrams indicate, the interaction 60–25 will necessarily generate a small degree of Mo–C(O)–Ru bridging character. Although much less important, the same is true of interaction 59–25. That the evolution of an Mo–C(O)–Ru bridging interaction is observed even when the molybdenum carbonyl ligands are essentially linear and terminal[20] in nature is a significant finding. The contribution (39%) made to the total interfragment bonding by the π interactions involving MO 26 of the $\{(cp)Mo(CO)_2\}^+$ fragment is consistent with the important role played by π interactions in main-group element capped clusters with a core M_3E (E = B or C).[42]

Solution Spectroscopic Data for Compound **7**.—As mentioned earlier, a partial solid-state structural determination for **7** confirms the presence of a trigonal-bipyramidal heavy-atom core and shows that the two tungsten atoms occupy equivalent equatorial sites. If this structure were to persist in solution we would expect to observe a single resonance in the ^{1}H NMR spectrum corresponding to the cp protons. In fact a sample of crystals of **7**, redissolved in CD_2Cl_2, exhibits two cp resonances of approximately 1:1.5 intensity at both 295 and 193 K. The signals shift slightly with temperature (295 K, δ 5.55, 5.50; 193 K, δ 5.50, 5.45) but the relative intensities remain as at room temperature. These data are inconsistent with the solid-state structural data but may be rationalized as follows. In theory, three isomeric forms of **7** are possible, each containing a trigonal-bipyramidal Ru_3W_2 core (Scheme 5); isomer **A** is that confirmed by single-crystal X-ray diffraction. Isomer **B** possesses two inequivalent tungsten sites and, as the sole or dominant solution species, would be consistent with the observed ^{1}H NMR spectroscopic data. Alternatively, the solution data are consistent with a mixture of isomers **A** and **C** present in proportions of 1:1.5. In view of the apparent temperature-invariant ^{1}H NMR spectrum of **7** and in the light of the bonding rationale presented earlier, we consider that it is more likely that isomer **B** predominates in solution, with the crystallographically confirmed isomer **A** being present in minor (≈20%) amounts; this explanation requires the not altogether unreasonable coincidence between resonances for the equatorially sited cp rings in isomers **A** and **B**.

Molecular Structure of Compound **5**.—The molecular structure of and labelling scheme for compound **5** are shown in Fig. 5, atomic coordinates are given in Table 5 and selected bond distances and angles are listed in Table 6. Compound **5** is the first heterometallic tetrametal butterfly cluster containing a semi-interstitial boron atom to be structurally characterized. The core structure of **5** differs from that of the carbido cluster $[WFe_3(CO)_{13}C]^{2-}$ as well as the related $[CrFe_3(CO)_{13}C]^{2-}$,

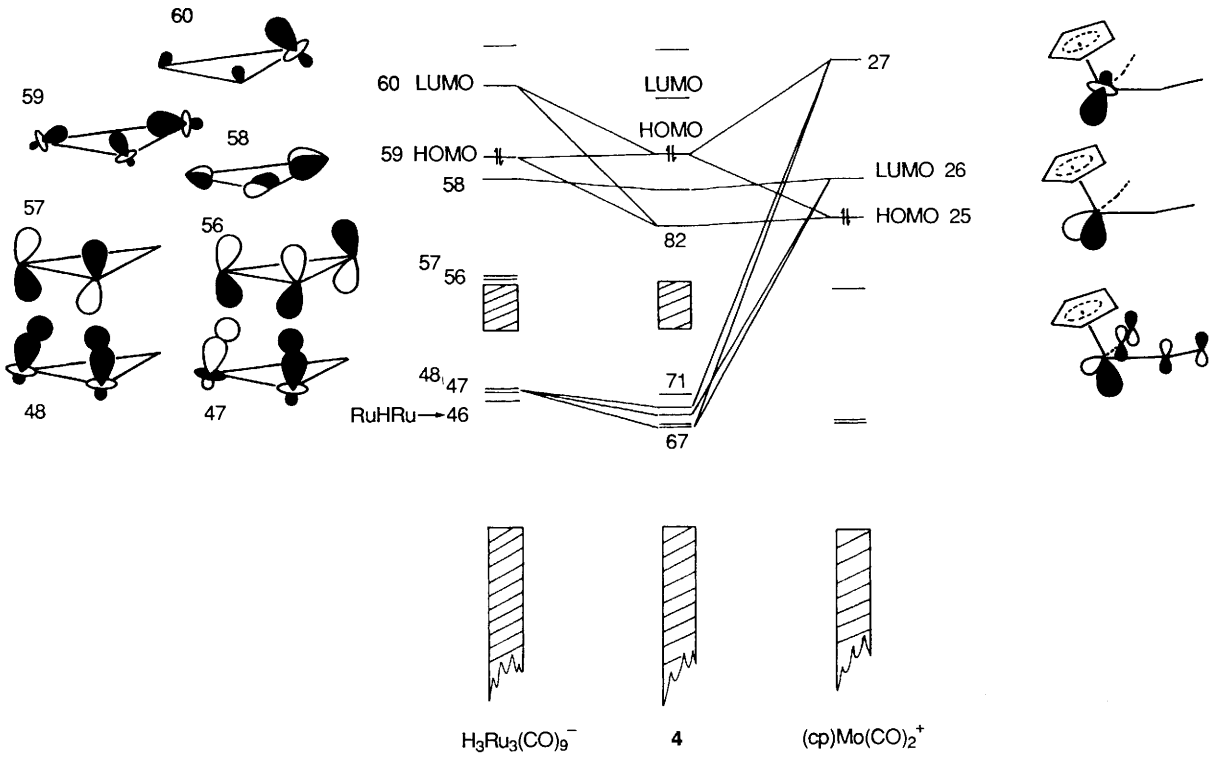

Fig. 4 Molecular orbital correlation diagram for the formation of $[MoRu_3(cp)H_3(CO)_{11}]$ **4** with isomer **I** structure from $\{H_3Ru_3(CO)_9\}^-$ and $\{(cp)Mo(CO)_2\}^+$ fragments. The frontier MOs of the two fragments are drawn schematically

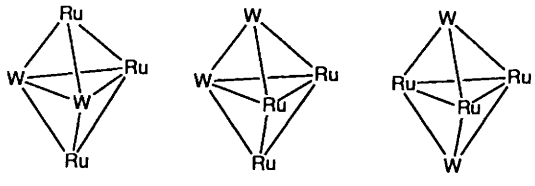

Scheme 5

Table 4 Mulliken overlap populations between the MOs of fragments $\{H_3Ru_3(CO)_9\}^-$ and $\{(cp)Mo(CO)_2\}^+$ used to generate compound **4**. Degenerate pairs of MOs are considered together. Each MOP is expressed (in parentheses) as a percentage of the total interfragment overlap population

Fragment MOs for $\{H_3Ru_3(CO)_9\}^-$	Fragment MOs for $\{(cp)Mo(CO)_2\}^+$		
	25 (HOMO)	26 (LUMO)	27
47/48		0.066 (17)	0.020 (5)
56/57		0.019 (5)	0.012 (3)
58		0.065 (17)	
59 (HOMO)	0.017 (4)		0.039 (10)
60 (LUMO)	0.112 (28)		0.044 (11)

HOMO = Highest occupied molecular orbital, LUMO = lowest occupied molecular orbital.

$[MnOs_3(CO)_{13}C]^-$, $[MnFe_3(CO)_{13}C]^-$ and $[RhFe_3(CO)_{12}C]^-$ in that the heterometal occupies a butterfly wingtip site in **5** but a hinge site in each of the carbido species.[2–6] The three ruthenium atoms in **5** retain the triangular framework present in the precursor **1**: Ru(1)–Ru(2) 2.833(5), Ru(2)–Ru(3) 2.825(5) and Ru(1)–Ru(3) 2.841(6) Å. Each ruthenium atom has attached to it three terminal carbonyl ligands which are unexceptional. The internal dihedral angle of the WRu_3 butterfly in **5** is 111.0° and this compares with values of 118, 116.1 and 117.4° in $[Ru_4H(CO)_{12}(BH_2)]$,[14] $[\{Ru_4H(CO)_{12}(BH)\}_2Au]^-$[43] and $[Ru_4H(CO)_{12}BAu_2(PPh_3)_2]$,[13] respectively.

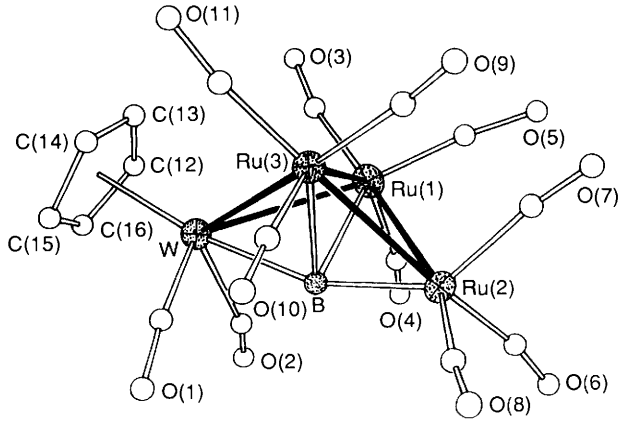

Fig. 5 Molecular structure and labelling scheme for compound **5**

The cluster hydride ligands in compound **5** were not located directly by X-ray crystallography. A consideration of the required cluster electron count of 62 electrons indicates that two hydrogen atoms must be associated with the cluster core. In the ^1H NMR spectrum of **5** [Fig. 6(*a*)] resonances at δ −6.6 (collapsed quartet) and −20.4 (sharp) indicate the presence of a bridging hydrogen atom attached to the boron atom and a metal hydride respectively. The ^{11}B NMR spectrum is shown in Fig. 6(*b*); a doublet at δ +131.9 ($J_{BH} \approx 65$ Hz) gives rise to a singlet upon proton decoupling. Inspection of the molecular structure of **5** in Fig. 5 illustrates that the two cluster hydride ligands may bridge edges Ru(2)–B and Ru(1)–Ru(3). The carbonyl ligands on atom Ru(2) are oriented such that the vector O(7)C(7)Ru(2) points to a space in the ligand shell in

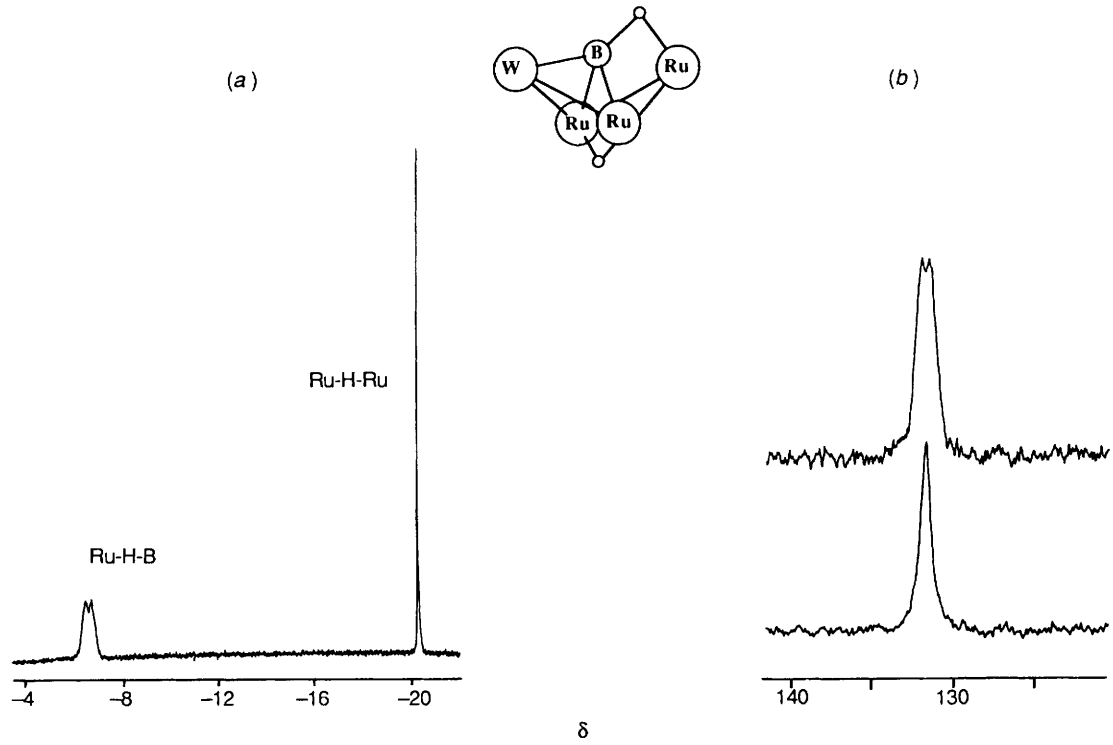

Fig. 6 NMR spectra of compound **5** in $CDCl_3$: (*a*) 250 MHz ^1H in the high-field region; (*b*) 128 MHz ^{11}B (upper) and ^{11}B-{^1H} (lower)

Table 5 Atomic coordinates (heavy atoms $\times 10^4$, light atoms $\times 10^3$) for $[WRu_3(cp)H(CO)_{11}(BH)]$ **5**

Atom	*x*	*y*	*z*
W	6483(1)	3586(2)	−996(1)
Ru(1)	7270(2)	3338(5)	848(2)
Ru(3)	8341(2)	3009(4)	15(2)
Ru(2)	8466(2)	5991(4)	992(2)
O(1)	697(2)	654(5)	−194(3)
O(2)	544(2)	653(4)	−72(2)
O(3)	618(4)	−7(7)	64(3)
O(4)	616(2)	598(5)	114(3)
O(5)	830(3)	275(5)	270(3)
O(6)	803(3)	871(5)	205(3)
O(7)	990(3)	439(8)	246(3)
O(8)	972(2)	821(4)	60(2)
O(9)	1013(2)	197(5)	122(2)
O(10)	903(3)	515(7)	−102(2)
O(11)	815(3)	−45(5)	−91(2)
B	743(4)	527(8)	−4(4)
C(1)	675(3)	524(7)	−158(3)
C(2)	592(4)	574(7)	−70(3)
C(3)	653(3)	130(6)	64(3)
C(4)	660(4)	517(8)	110(4)
C(5)	787(3)	287(6)	192(3)
C(6)	829(3)	761(6)	69(3)
C(7)	934(4)	484(8)	191(4)
C(8)	922(4)	742(8)	70(4)
C(9)	948(3)	240(5)	81(2)
C(10)	866(3)	426(6)	−62(3)
C(11)	819(3)	99(6)	−60(3)
C(12)	541(4)	158(8)	−135(4)
C(13)	615(3)	68(7)	−128(3)
C(14)	635(4)	115(7)	−183(3)
C(15)	572(4)	246(9)	−235(4)
C(16)	512(4)	265(7)	−203(3)

which one hydrogen atom may be accommodated. Similarly, the carbonyl ligands on atoms Ru(1) and Ru(3) are bent away from the metal–metal edge.

Table 6 Selected bond distances (Å) and angles (°) for $[WRu_3(cp)H(CO)_{11}(BH)]$ **5**

W–Ru(1)	3.003(4)	W–Ru(3)	2.987(3)
W–B	2.21(6)	Ru(1)–Ru(3)	2.841(6)
Ru(1)–Ru(2)	2.833(5)	Ru(1)–B	2.27(7)
Ru(3)–Ru(2)	2.825(5)	Ru(3)–B	2.32(7)
Ru(2)–B	2.04(6)		
Ru(1)–W–Ru(3)	56.6(1)	Ru(1)–W–B	48.9(19)
Ru(3)–W–B	50.3(18)	W–Ru(1)–Ru(3)	61.4(1)
W–Ru(1)–Ru(2)	91.7(1)	Ru(3)–Ru(1)–Ru(2)	59.7(1)
W–Ru(1)–B	47.1(14)	Ru(3)–Ru(1)–B	52.5(19)
Ru(2)–Ru(1)–B	45.6(14)	W–Ru(3)–Ru(1)	62.0(1)
W–Ru(3)–Ru(2)	92.2(1)	Ru(1)–Ru(3)–Ru(2)	60.0(1)
W–Ru(3)–B	47.2(14)	Ru(1)–Ru(3)–B	51.1(19)
Ru(2)–Ru(3)–B	45.5(14)	Ru(1)–Ru(2)–Ru(3)	60.3(1)
Ru(1)–Ru(2)–B	52.6(20)	Ru(3)–Ru(2)–B	54.1(19)
W–B–Ru(1)	84.0(23)	W–B–Ru(3)	82.4(22)
W–B–Ru(2)	160(3)	Ru(1)–B–Ru(3)	76.4(20)
Ru(1)–B–Ru(2)	81.8(21)	Ru(2)–B–Ru(3)	80.4(21)

The spectral properties of compound **3** indicate that it has an analogous molecular structure to that of **5**. In both compounds the cluster hydrogen atoms are static in solution on the NMR time-scale.

Conclusions

The results reported here illustrate that, not only are the ruthenaboranes **1** and **2** suitable precursors for the generation of heterometalloboranes, they are also able to function as a source of a 'superunsaturated' triruthenium framework. Although **1** and **2** are readily described as clusters and obey polyhedral skeletal electron pair theory, the reactions summarized in Scheme 2 are not all easily rationalized in terms of cluster principles. Both **1** and **2** are conveniently considered in terms of a mono- or di-borane ligand interacting with a triruthenium framework. Further investigations of the reactivity of compounds **1** and **2** and of the heterometallic clusters **3** and **5** are in progress.

Acknowledgements

We thank the donors of the Petroleum Research Fund, administered by the American Chemical Society, for support of this work (grant no. 22771-AC3), the SERC for a studentship (to D. M. M.), the Issac Newton Trust (to X. S.) and the NSF for a grant (CHE 9007852) towards the purchase of a diffractometer at the University of Delaware. Johnson-Matthey is thanked for generous loans of $RuCl_3$.

References

1 C. E. Housecroft, *Adv. Organomet. Chem.*, 1991, **33**, 1.
2 J. A. Hriljac, S. Harris and D. F. Shriver, *Inorg. Chem.*, 1988, **27**, 816.
3 J. A. Hriljac, P. N. Swepston and D. F. Shriver, *Organometallics*, 1985, **4**, 158.
4 J. W. Kolis, E. M. Holt, J. A. Hriljac and D. F. Shriver, *Organometallics*, 1984, **3**, 496.
5 J. A. Hriljac, E. M. Holt and D. F. Shriver, *Inorg. Chem.*, 1987, **26**, 2943.
6 M. P. Jensen, W. Henderson, D. H. Johnston, M. Sabat and D. F. Shriver, *J. Organomet. Chem.*, 1990, **394**, 121.
7 C. K. Schauer and D. F. Shriver, *Angew. Chem., Int. Ed. Engl.*, 1987, **26**, 255.
8 S. M. Draper, C. E. Housecroft, A. K. Keep, D. M. Matthews, X. Song and A. L. Rheingold, *J. Organomet. Chem.*, 1992, **423**, 241.
9 C. E. Housecroft and T. P. Fehlner, *Organometallics*, 1986, **5**, 379.
10 C. E. Housecroft, M. L. Buhl, G. J. Long and T. P. Fehlner, *J. Am. Chem. Soc.*, 1987, **109**, 3323.
11 A. K. Chipperfield and C. E. Housecroft, *J. Organomet. Chem.*, 1988, **349**, C17.
12 C. R. Eady, B. F. G. Johnson and J. Lewis, *J. Chem. Soc., Dalton Trans.*, 1977, 477.
13 A. K. Chipperfield, C. E. Housecroft and A. L. Rheingold, *Organometallics*, 1990, **9**, 681.
14 F.-E. Hong, D. A. McCarthy, J. P. White III, C. E. Cottrell and S. G. Shore, *Inorg. Chem.*, 1990, **29**, 2874.
15 K. Wade, *Adv. Inorg. Chem. Radiochem.*, 1976, **18**, 1.
16 A. K. Chipperfield, C. E. Housecroft and D. M. Matthews, *J. Organomet. Chem.*, 1990, **384**, C38.
17 C. E. Housecroft, D. M. Matthews and A. L. Rheingold, *J. Chem. Soc., Chem. Commun.*, 1992, 323.
18 M. I. Bruce, C. M. Jensen and N. L. Jones, *Inorg. Synth.*, 1989, **26**, 259.
19 S. R. Drake and R. Khattar, in *Organometallic Syntheses*, eds. R. B. King and J. J. Eisch, Elsevier, Amsterdam, 1988, vol. 4, p. 234.
20 Y. Chi, C.-Y. Cheng and S.-L. Wang, *J. Organomet. Chem.*, 1989, **378**, 45.
21 G. M. Sheldrick, SHELXTL 5.1, Nicolet (Siemens), Madison, WI.
22 M. B. Hall and R. F. Fenske, *Inorg. Chem.*, 1972, **11**, 768.
23 E. Clementi, *J. Chem. Phys.*, 1964, **40**, 1944.
24 J. W. Richardson, M. J. Blackman and J. F. Ranochak, *J. Chem. Phys.*, 1973, **58**, 3010.
25 N. M. Kostic and R. F. Fenske, *Organometallics*, 1982, **1**, 974.
26 L.-H. Hsu, W.-L. Hsu, D.-Y. Jan and S. G. Shore, *Organometallics, 1986*, **5**, 1041.
27 See, for example, C. E. Housecroft and T. P. Fehlner, *Adv. Organomet. Chem.*, 1982, **21**, 57.
28 T. P. Fehlner, in *Boron Chemistry*, eds. R. W. Parry and G. Kodama, Pergamon, Oxford, 1980, p. 95.
29 T. P. Fehlner, *Adv. Inorg. Chem.*, 1990, **35**, 199.
30 N. N. Greenwood, C. G. Savory, R. N. Grimes, L. G. Sneddon, A. Davison and S. S. Wreford, *J. Chem. Soc., Chem. Commun.*, 1974, 718.
31 V. R. Miller and R. N. Grimes, *J. Am. Chem. Soc.*, 1973, **95**, 5078.
32 V. R. Miller and R. N. Grimes, *J. Am. Chem. Soc.*, 1976, **98**, 1600.
33 V. R. Miller, R. Weiss and R. N. Grimes, *J. Am. Chem. Soc.*, 1977, **99**, 5646.
34 L. G. Sneddon and D. Voet, *J. Chem. Soc., Chem. Commun.*, 1976, 118.
35 E. L. Andersen, K. J. Haller and T. P. Fehlner, *J. Am. Chem. Soc.*, 1979, **101**, 4390.
36 K. J. Haller, E. L. Andersen and T. P. Fehlner, *Inorg. Chem.*, 1981, **20**, 309.
37 K. S. Wong, W. R. Scheidt and T. P. Fehlner, *J. Am. Chem. Soc.*, 1982, **104**, 1111.
38 T. P. Fehlner, C. E. Housecroft, W. R. Scheidt and K. S. Wong, *Organometallics*, 1983, **2**, 825.
39 M. R. Churchill, F. J. Hollander, J. R. Shapley and D. S. Foose, *J. Chem. Soc., Chem. Commun.*, 1978, 534.
40 M. R. Churchill and F. J. Hollander, *Inorg. Chem.*, 1979, **18**, 161.
41 M. Cazanoue, N. Lugan, J.-J. Bonnet and R. Mathieu, *Organometallics*, 1988, **7**, 2480.
42 M. M. Lynam, D. M. Chipman, R. D. Barreto and T. P. Fehlner, *Organometallics*, 1987, **6**, 2405.
43 S. M. Draper, C. E. Housecroft, J. E. Rees, M. S. Shongwe, B. S. Haggerty and A. L. Rheingold, *Organometallics*, 1992, **11**, 2356.

Received 21*st January* 1992; *Paper* 2/00342B